Pergamon

Cement and Concrete Research 30 (2000) 1121–1129

CEMENT AND CONCRETE RESEARCH

Influence of silica fume on diffusivity in cement-based materials II. Multi-scale modeling of concrete diffusivity

D.P. Bentz*

Building and Fire Research Laboratory, National Institute of Standards and Technology, 100 Bureau Drive Stop 8621, Gaithersburg, MD 20899-8621, USA

Received 19 November 1999; accepted 14 February 2000

Abstract

Based on a set of multi-scale computer models, an equation is developed for predicting the chloride ion diffusivity of concrete as a function of water-to-cement (w/c) ratio, silica fume addition, degree of hydration and aggregate volume fraction. Silica fume influences concrete diffusivity in several ways: (1) densifying the microstructure of the interfacial transition zone (ITZ) regions, (2) reducing the overall (bulk and ITZ) capillary porosity for a fixed degree of cement hydration, and (3) producing a pozzolanic C-S-H gel with a relative diffusivity about 25 times less than that of the C-S-H gel produced from conventional cement hydration. According to the equation and in agreement with results from the literature, silica fume is most efficient for reducing diffusivity in lower w/c ratio concretes (w/c < 0.4). In these systems, for moderate additions of silica fume (e.g., 10%), the reduction in concrete diffusivity may be a factor of 15 or more, which may substantially increase the service life of steel-reinforced concrete exposed in a severe corrosion environment.

Keywords: Concrete; Diffusion; Hydration; Modeling; Silica fume

1. Introduction

One key parameter influencing the service life of a concrete structure is the diffusivity of the concrete [1]. In many cases, the rate of ingress of some deleterious species such as chloride or sulfate ions regulates the initiation of deterioration. In the 1990s, much research and development has been conducted to produce more durable (so-called high performance) concretes. It has been recognized that strength and durability are different properties of a concrete, and that the transport properties of the "covercrete" (the top exposed layer of the concrete) are particularly vital in determining its durability and service life.

In the 1970s, the Nordic countries initiated the incorporation of condensed silica fume (CSF) into concrete to produce higher strengths [2]. Silica fume also offers many potential durability benefits (although its tendency to increase autogenous deformation [3], adiabatic temperature rise [4], and early-age cracking must be carefully controlled). Measurements of the diffusivity of concrete with and without silica fume [5–7] based on the rapid chloride permeability test [8] or on more direct measurements of chloride ingress have all indicated a substantial reduction in diffusivity for the concretes containing silica fume. In this paper, a set of multi-scale computer models is used to develop an equation for predicting the diffusivity of a concrete containing silica fume based on four inputs: the water-to-cement ratio (w/c), the silica fume addition, the volume fraction of aggregates and the degree of hydration of the cement. Previously, these techniques have been applied to ordinary concrete and mortar with no mineral admixtures [9,10], and here are extended to concretes with silica fume, based on recent experimental and computer modeling results on the influence of silica fume on the diffusivity of cement pastes [11].

2. Computer modeling

The multi-scale modeling approach used here to predict concrete diffusivity has been outlined previously [9]. It is based on the combination of a cellular-automaton-based three-dimensional model for cement paste hydration and microstructure development [12] and a three-dimensional

* Tel.: +1-301-975-5865; fax: +1-301-990-6891.
E-mail address: dale.bentz@nist.gov (D.P. Bentz).

0008-8846/00/$ – see front matter
PII: S0008-8846(00)00263-5

hard core/soft shell (HCSS) model for concrete [13]. The approach follows these steps.

(1) The "median" cement particle diameter is used to establish the thickness of the interfacial transition zone (t_{ITZ}) surrounding each aggregate.
(2) The HCSS model is executed for the volume fraction and particle size distribution (PSD) of aggregate and t_{ITZ} of interest to determine the volume fractions of bulk (V_{bulk}) and ITZ (V_{ITZ}) cement paste (alternately, the analytical equations of Lu and Torquato [14] and Garboczi and Bentz [15] can be used for this determination).
(3) These paste fractions are duplicated in the cement paste microstructural model in a system containing a single flat plate aggregate with the desired cement PSD, overall w/c ratio, and silica fume addition.
(4) Hydration of the cement paste microstructure is simulated for a fixed number of cycles or until a degree of hydration of interest.
(5) The hydrated microstructure is analyzed to determine the capillary porosity present in the cement paste as a function of distance from the aggregate surface.
(6) These local porosities and the initial local silica fume addition are substituted into a previously developed equation relating relative diffusivity of cement paste to capillary porosity and silica fume addition [11].
(7) The local relative diffusivities are averaged into two subsets—those within the ITZ region and those within the bulk cement paste.
(8) The ratio of "average" ITZ diffusivity (D_{ITZ}) to average bulk cement paste diffusivity (D_{bulk}) is computed and used as input back into the HCSS model to determine the effective diffusivity of the concrete composite (D_{eff}) relative to the average value for the bulk cement paste (using random walker techniques [16], typically with 10,000 random walkers each taking on the order of 1,000,000 random steps).
(9) the overall diffusivity of the concrete is computed by multiplying the result of step (8) by the average bulk cement paste relative diffusivity determined in step (7) and by the diffusivity of chloride ions in bulk water (taken to be 1.81×10^{-9} m^2/s at 20°C [17], for this study).

The cement paste–single aggregate microstructural model was executed at a resolution of 1 μm/pixel with system sizes ranging from $170 \times 170 \times 170$ pixels to $234 \times 234 \times 234$ pixels depending on the specific value of V_{ITZ}/V_{bulk}. The system volume for the concrete microstructural model was a cube 3-cm on a side. Both models employed periodic boundary conditions to eliminate artificial edge effects.

The cement used in all of the computer experiments had the following composition on a volume basis: C_3S—0.665, C_2S—0.1425, C_3A—0.095, C_4AF—0.0475, and gypsum—0.05. Its PSD corresponded to that of a cement with a measured Blaine fineness of 387 m^2/kg and a Rosin–Rammler mean particle diameter of approximately 15 μm [18]. The silica fume (specific gravity of 2.2) is modeled as 1-pixel particles, 1 μm in diameter. To simulate "good" curing conditions, the cement hydration model was executed under saturated conditions until the capillary porosity depercolated and under sealed conditions thereafter. Under sealed conditions, the appropriate empty capillary pores are created to account for the chemical shrinkage occurring during cement hydration [12,19]. The aggregate PSD corresponded to the midpoint of the upper and lower limits given in ASTM C33 [20] for coarse (maximum diameter of 19.0 mm) and fine aggregates [9]. This resulted in approximately 500,000 aggregates being present in the 27,000 mm^3 concrete computational cell.

For the computer experiment, the following variables and settings were examined in a full factorial experimental design:

w/c	0.3	0.4	0.5
CSF addition (mass fraction of cement basis)	0.00	0.05	0.10
V_{agg} (volume fraction of aggregates)	0.62	0.70	
Cycles of hydration	850	2000	

The total number of computer experiments was thus 36 ($= 3 \times 3 \times 2 \times 2$). The hydration model was executed for fixed numbers of cycles (times) instead of fixed degrees of hydration because the ultimately obtainable degree of hydration is a function of the w/c ratio. A total of 850 cycles should be fairly typical of 28 days of room temperature curing, while 2000 cycles should correspond to approximately 180 days of curing.

The results were analyzed using ordinary least squares regression analysis [21]. Including only the interaction effects (second order cross product terms) that were determined to be significant, the base 10 logarithm of the concrete diffusivity, D_{conc}, was fit to a function of the form:

$$\log_{10}(D_{conc}) = a_0 + a_1\left(\frac{w}{c}\right) + a_2\left(\frac{w}{c}\right)^2 + a_3\mathrm{CSF} + a_4(\mathrm{CSF})^2 + a_5\left(\frac{w}{c}\right)\mathrm{CSF} + a_6\alpha + a_7\left(\frac{w}{c}\right)\alpha + a_8(\mathrm{CSF})\alpha + a_9 V_{agg} \quad (1)$$

where CSF is the silica fume addition rate, α is the degree of hydration of the cement, and a_0 to a_9 are the fitting coefficients. For the settings examined in this study, all four independent variables will have values between 0 and 1. Viewing this equation, it can be seen that, specifically, the interaction effects between the volume fraction of aggregates, V_{agg}, and each of the other three variables were determined to be insignificant based on the regression analysis of the results presented below.

3. Results and discussion

Silica fume influences the microstructural development of hydrating cement paste in concrete through at least three

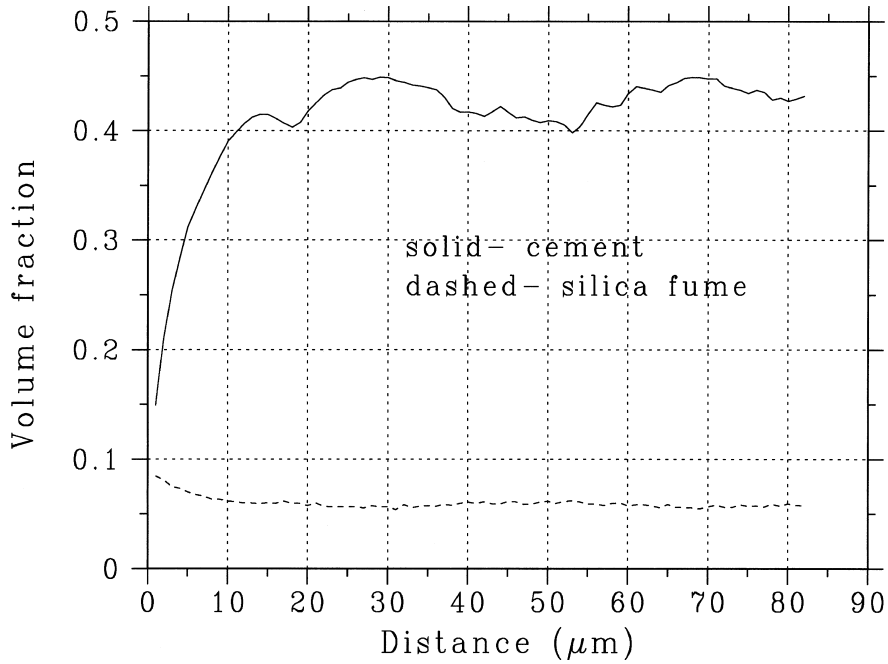

Fig. 1. Model results for initial cement and silica fume volume fractions vs. distance from center of aggregate surface for a w/c = 0.4 concrete with 10% silica fume addition on a mass basis. Note that the ITZ is seen to extend approximately 15 μm into the cement paste, corresponding to the "median" cement particle diameter.

mechanisms. First, because of its small particle size, silica fume packs more efficiently in the ITZ region than the larger cement particles do. This is illustrated in Fig. 1, which plots the variation in volume fraction of cement and silica fume (for a unit cement paste basis) with distance from the single aggregate surface for an initial microstructure, for a concrete with w/c = 0.4 and a 10% silica fume addition on a mass basis. When viewing Fig. 1, it should be kept in mind that the results shown are for packing digitized "spherical" particles, and that in continuum space, even the volume

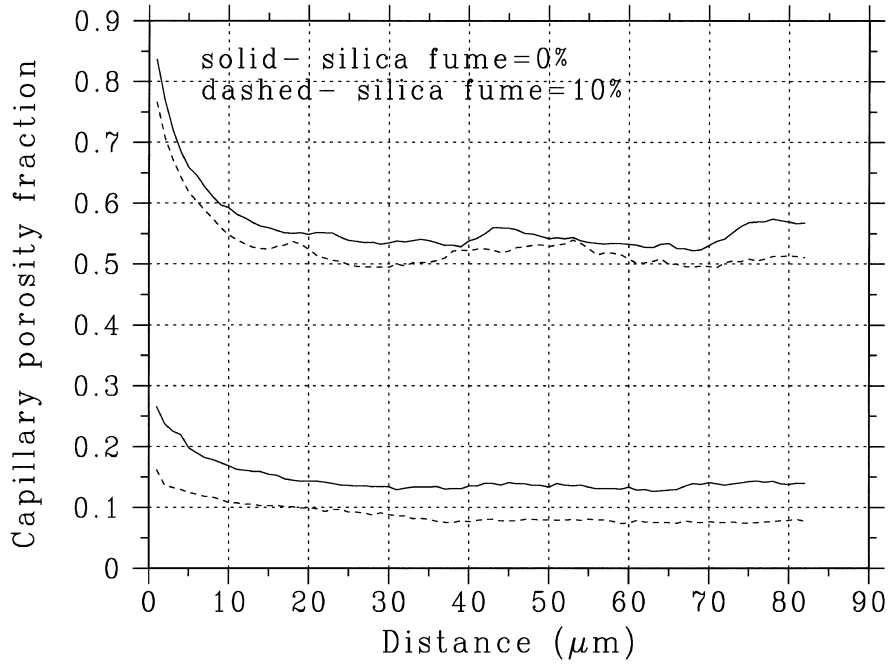

Fig. 2. Model results for capillary porosity fraction (in the cement paste) vs. distance from center of aggregate surface for w/c = 0.4 concretes hydrated for 2000 cycles using the NIST model. Top two lines indicate initial capillary porosities and the lower two correspond to capillary porosities after hydration.

fraction of the much smaller silica fume would decrease within 1 μm or so of the aggregate surface (due to inefficient packing of spheres against a "flat" wall).

Due to these packing limitations, the cement volume fraction is seen to decrease significantly as the aggregate surface is approached, so that the water volume fraction naturally increases. The very fine silica fume particles are more or less evenly distributed within this water phase and therefore, actually exhibit an increase in volume fraction in the ITZ relative to the bulk paste. Thus, the ratio of silica fume to cement is much higher in the ITZ region than it is in the bulk paste. This "extra" silica fume in the ITZ region will participate in pozzolanic reactions, resulting in a denser, more homogeneous ITZ microstructure [22].

Second, silica fume reduces the overall porosity in a concrete. These first two effects of silica fume can be clearly seen in Fig. 2, which contrasts the variation in capillary porosity in the cement paste with distance from the surface of an aggregate particle for w/c = 0.4 systems with silica fume additions of 0% and 10%. Because we are considering a silica fume addition, the initial overall porosity is slightly reduced due to the additional volume occupied by the silica fume. Still, after hydration, the overall porosity is further reduced, due to the pozzolanic reaction. Furthermore, the porosity gradient in the ITZ region is also significantly reduced. This improvement in microstructure is achieved despite the fact that after 2000 cycles of hydration, the degree of hydration of the cement in the 0% silica fume system is 0.843, while that in the one with 10% silica fume is only 0.775 (due to water availability/space limitations).

Silica fume has a third extremely significant effect on the microstructure of hydrating cement paste. The pozzolanic C-S-H gel produced from silica fume appears to have an inherent chloride ion diffusivity that is approximately 25 times less than that of C-S-H gel formed from conventional cement hydration [11]. In part I of this paper [11], the following equation was developed for estimating the relative diffusivity of a cement paste with silica fume as a function of capillary porosity, ϕ, and silica fume content, CSF:

$$\frac{D}{D_0}(\phi, \mathrm{CSF}) = \frac{0.0004}{\beta(\mathrm{CSF})} + \frac{0.03}{\beta(\mathrm{CSF})}\phi^2 + 1.7(\phi - \phi_c)^2 H(\phi - \phi_c) \quad (2)$$

where D is the diffusivity of chloride ions in the cement paste, D_0 is their corresponding diffusivity in bulk water, ϕ_c is the capillary porosity at which the capillary pore space depercolates (0.17), H is the Heaviside function ($H(x) = 1$ when $x > 0$ and 0 otherwise), and β(CSF) is a function of the silica fume addition that can be approximated by:

$$\beta(\mathrm{CSF}) = 1.0 \qquad \mathrm{CSF} \leqq 0.025$$

$$\beta(\mathrm{CSF}) = 1.0 - 48.6 \cdot \mathrm{CSF} + 2330 \cdot (\mathrm{CSF})^2 - 11400 \cdot (\mathrm{CSF})^3 \qquad 0.025 < \mathrm{CSF} \leqq 0.12 \quad (3)$$

$$\beta(\mathrm{CSF}) = 9.0 \qquad \mathrm{CSF} > 0.12.$$

β represents the reduction in diffusivity of the C-S-H gel component of the cement paste due to the formation of a pozzolanic C-S-H gel with an inherent diffusivity lower than that of primary C-S-H gel formed during conventional cement hydration [11]. The upper bound value of 9.0 for silica fume

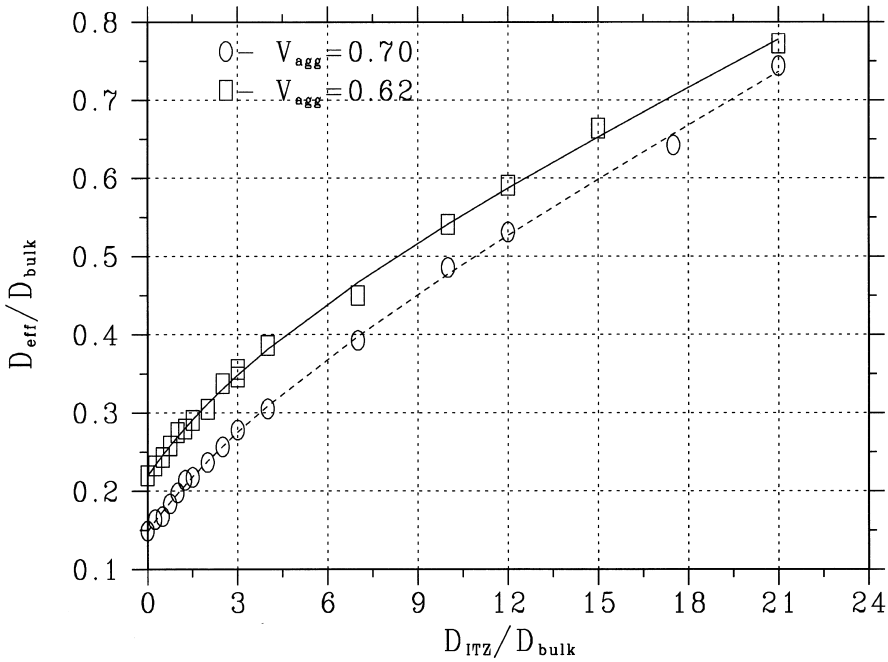

Fig. 3. Ratio of $D_{\mathrm{eff}}/D_{\mathrm{bulk}}$ vs. $D_{\mathrm{ITZ}}/D_{\mathrm{bulk}}$ for aggregate volume fractions of 0.62 and 0.70. Solid and dashed lines are fits of Eq. (4) to the simulation data points.

additions greater than 12% is a conservative estimate, as the experimental data of Jensen [17] indicates further significant improvements in performance for silica fume additions up to 20% (which are not explained by the current versions of the microstructural models [11]). This is not an issue for the 5% silica fume additions where the *local* silica fume content rarely exceeds 10%, but is an issue for the overall silica fume additions of 10%, where the average silica fume content in the ITZ regions may slightly exceed 16%. Because we have taken a conservative approach, our predictions of the improvements due to silica fume will be lower bounds on what may actually be experienced in practice.

At the concrete level, it is necessary to determine the influence of the increased ITZ diffusivity on the overall diffusivity of the concrete composite. Rather than executing the concrete level HCSS model for each of the 36-computer experiment runs, the ratio of D_{ITZ}/D_{bulk} was varied systematically for both of the aggregate volume fractions being considered in this study. Because of the densifying nature of silica fume on ITZ microstructure, it was necessary to execute the HCSS model for cases both where the ITZ region had an enhanced diffusivity relative to that of the bulk cement paste ($D_{ITZ}/D_{bulk} > 1$) and vice versa ($D_{ITZ}/D_{bulk} < 1$). Fig. 3 shows the values obtained for the ratio of D_{eff} to D_{bulk} for the various values of D_{ITZ}/D_{bulk}. Previously, Garboczi et al. [16] have shown that such data can be described by a relationship of the form:

$$\frac{D_{eff}}{D_{bulk}} = \frac{a + bX + cX^2}{1 + dX} \tag{4}$$

where X is the ratio D_{ITZ}/D_{bulk}. This equation was fitted to the two data sets shown in Fig. 3; the resulting coefficients are provided in Table 1. It is clear from the coefficients in Table 1 and the data in Fig. 3 that, all other things being equal, an increase in aggregate volume fraction will result in a decrease in concrete diffusivity for the aggregate gradation and ITZ thickness examined in this study, in agreement with the experimental results of Buenfeld and Okundi [23] for a limited set of concretes. Of course, this computer study neglects the effects of segregation, bleeding, and improper consolidation, all of which could lead to increased diffusivities as the volume fraction of aggregates is increased in ''real-world'' concretes.

The diffusivity results obtained for the 36 different concrete mixtures are summarized in Table 2. The final values for D_{conc} are seen to span nearly three orders of magnitude. When examining the variation of the ratio D_{ITZ}/D_{bulk} with respect to the independent variables, interestingly, for lower w/c ratios, this ratio generally decreases with increasing hydration, while for w/c = 0.5, the converse is true. This is due to the specific nature of the relationship between capillary porosity and diffusivity (Eq. (2)). For a given cement paste system, the ratio of D_{ITZ}/D_{bulk} will rise to a maximum with increasing hydration (as the bulk capillary porosity depercolates before that contained in the ITZ regions), and then fall as both the ITZ and bulk paste capillary porosities become depercolated [10,24].

The values of D_{conc} given in Table 2 were fitted to the functional form provided in Eq. (1), resulting in the following predictive equation for concrete diffusivity as a function of mixture proportions and expected degree of hydration:

$$\begin{aligned}\log_{10}(D_{conc}) = {} & -13.75 - 0.82\left(\frac{w}{c}\right) + 32.55\left(\frac{w}{c}\right)^2 \\ & + 8.374\mathrm{CSF} + 15.36(\mathrm{CSF})^2 \\ & + 23.15\left(\frac{w}{c}\right)\mathrm{CSF} + 5.79\alpha \\ & - 21.10\left(\frac{w}{c}\right)\alpha - 43.15(\mathrm{CSF})\alpha - 1.705V_{agg}\end{aligned} \tag{5}$$

Table 1
Coefficients from fitting Eq. (4) to simulation data

V_{agg}	a	b	c	d
0.62	0.2195	0.09296	0.00317	0.1709
0.70	0.1483	0.07806	0.00353	0.1686

Table 2
Diffusion coefficients for the 36 concrete mixtures (t_{ITZ}=15 μm)

w/c	CSF (%)	α	V_{agg} (%)	D_{bulk}/D_0	D_{ITZ}/D_{bulk}	D_{conc} $\times 10^{-12}$ m^2/s
0.3	0	0.686	70	0.000641	1.29	0.243
0.3	0	0.746	70	0.000491	1.15	0.181
0.4	0	0.757	70	0.001580	6.81	1.123
0.4	0	0.843	70	0.000959	4.03	0.537
0.5	0	0.799	70	0.016700	3.02	8.334
0.5	0	0.876	70	0.008230	4.45	4.813
0.3	5	0.644	70	0.000199	0.69	0.066
0.3	5	0.688	70	0.000168	0.65	0.055
0.4	5	0.726	70	0.000387	3.64	0.208
0.4	5	0.799	70	0.000273	1.08	0.099
0.5	5	0.773	70	0.005500	3.49	2.906
0.5	5	0.857	70	0.000971	8.90	0.789
0.3	10	0.615	70	0.000063	0.97	0.022
0.3	10	0.655	70	0.000055	0.86	0.019
0.4	10	0.714	70	0.000112	4.43	0.065
0.4	10	0.775	70	0.000081	1.19	0.030
0.5	10	0.768	70	0.001640	6.79	1.164
0.5	10	0.845	70	0.000145	17.45	0.172
0.3	0	0.686	62	0.000662	1.26	0.337
0.3	0	0.755	62	0.000491	1.16	0.246
0.4	0	0.758	62	0.001850	5.07	1.386
0.4	0	0.844	62	0.001030	3.20	0.662
0.5	0	0.794	62	0.019300	2.23	11.190
0.5	0	0.877	62	0.009620	2.98	6.053
0.3	5	0.647	62	0.000193	0.68	0.089
0.3	5	0.690	62	0.000162	0.63	0.074
0.4	5	0.732	62	0.000378	4.87	0.279
0.4	5	0.809	62	0.000258	0.98	0.126
0.5	5	0.772	62	0.006850	3.13	4.374
0.5	5	0.853	62	0.001250	7.95	1.112
0.3	10	0.632	62	0.000061	0.98	0.030
0.3	10	0.669	62	0.000055	0.89	0.026
0.4	10	0.721	62	0.000114	2.90	0.071
0.4	10	0.785	62	0.000081	1.11	0.040
0.5	10	0.765	62	0.002380	4.90	1.761
0.5	10	0.842	62	0.000153	20.90	0.215

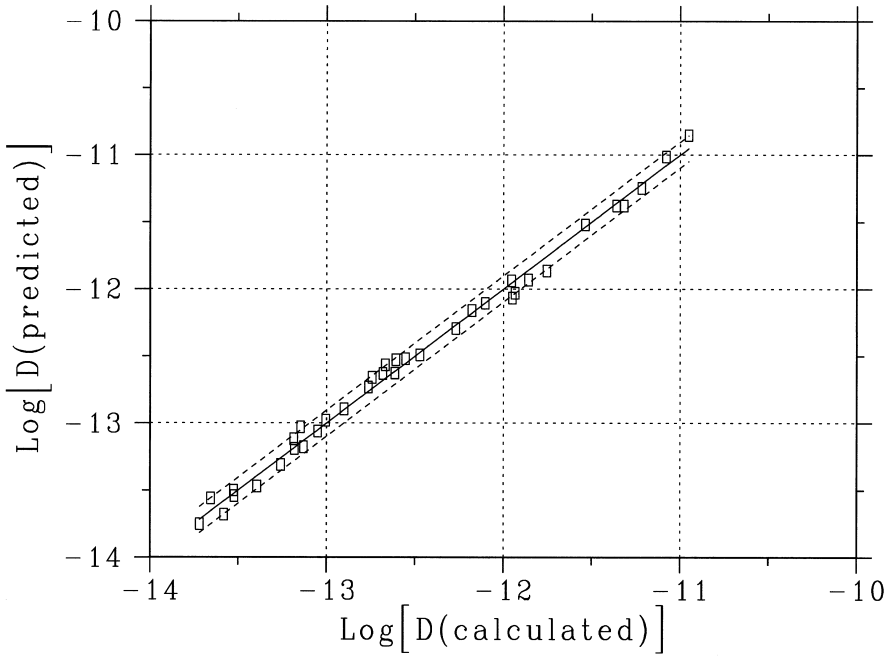

Fig. 4. Predicted vs. computed diffusion coefficients for the concretes examined in this computer experiment. Solid line indicates a one to one relation between predicted and calculated values. Dotted lines indicate a factor of 1.25 (25%) above and below the calculated values.

where D is in units of m^2/s. As shown in Fig. 4, which plots the predicted values vs. those obtained from the computer experiment, Eq. (5) generally predicts the simulated results within 25% of the actual value. This is considered to be a reasonable prediction considering that, as mentioned earlier, the simulated values span nearly three orders of magnitude.

Eq. (5) can also be used to predict the relative improvement in diffusion resistance offered by various addition levels of silica fume. This is most easily formulated as the

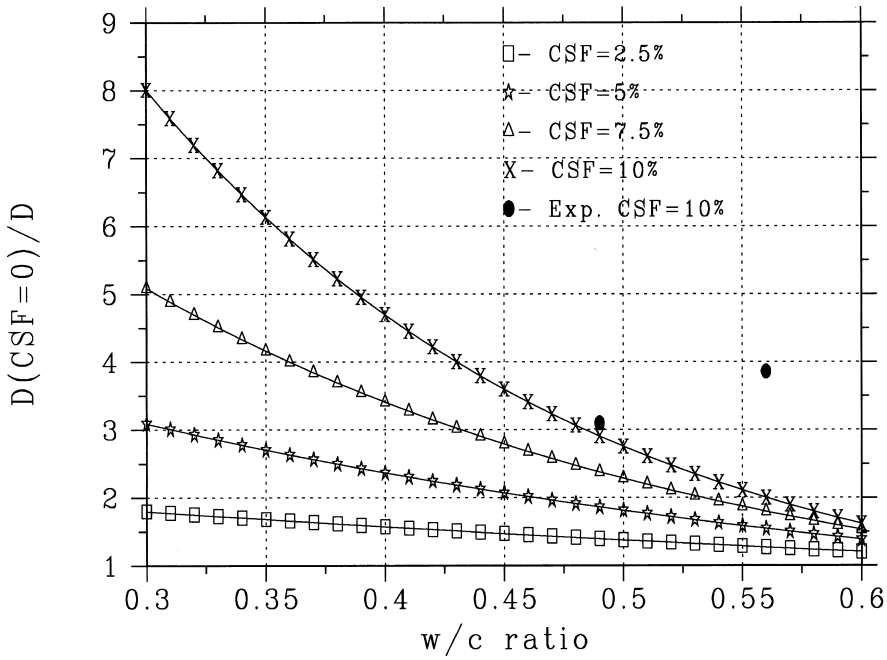

Fig. 5. Computed multiplicative increase in diffusion resistance due to silica fume addition vs. w/c ratio for an assumed degree of hydration of 0.6. Filled data points indicate the experimental data of Alexander and Magee [25].

multiplicative increase in diffusion resistance for a given silica fume addition (due to the logarithm form of Eq. (5)) and specific values of w/c ratio and degree of hydration. In this case, the multiplicative increase is given by:

$$\frac{D_{\text{conc}}(\text{CSF}=0)}{D_{\text{conc}}(\text{CSF})} = 10^{-\left[\left(8.374-43.15\alpha+23.15\left(\frac{w}{c}\right)\right)\text{CSF}+15.36(\text{CSF})^2\right]}. \quad (6)$$

Since both w/c and α are variables in Eq. (6), we will fix α and plot the variation in the dependent variable with w/c ratio for four different silica fume additions (2.5%, 5%, 7.5% and 10%). Figs. 5 and 6 provide examples of the results for $\alpha = 0.6$ and $\alpha = 0.675$, respectively. In both of these figures, it is clear that silica fume is more effective in reducing diffusivity in lower w/c ratio concretes. This is in agreement with the rapid chloride permeability measurements of Berke and Roberts [5]. For the lower w/c ratios (e.g., 0.3), the addition of 10% silica fume may decrease the chloride ion diffusivity by a factor of 15 or more.

A more quantitative evaluation against the experimental data can be made using the data sets of Hooton et al. [6] and of Alexander and Magee [25]. Hooton et al. [6] measured concrete diffusivity by a number of methods for three different water-to-cementitious materials (w/b) ratios and three different silica fume replacement levels. For comparison purposes, we shall consider their diffusion results generated in the long term, from a modified chloride ponding test. It is worth noting, however, that the relative improvement provided by the silica fume is nearly constant for all of the different "diffusion" coefficients measured in Ref. [6]. This, in spite of the fact, that for a given concrete, the different tests may produce results that vary by up to a factor of three [6]. Because in the current computer experiment, the w/c ratio is maintained constant and silica fume additions are considered, the experimental data reported in Ref. [6] must first be transformed to the same parameter space. Thus, the w/b = 0.35 mixture with a 12% silica fume replacement corresponds very closely to a w/c = 0.4 mixture with a 13.8% silica fume addition. Similarly, the w/b = 0.4 mixture with a 7% silica fume replacement corresponds to approximately a w/c = 0.44 mixture with a 7.7% silica fume addition. Alexander and Magee [25] measured the chloride conductivity of 28-day-old concretes with and without 10% silica fume additions, using a conductivity cell of their own design.

Of course, an estimate of the degree of hydration of the actual concretes evaluated is required; this will surely vary with w/c ratio and silica fume addition. For this comparison, the simplifying assumption was made that the degree of hydration of all of the concretes of Hooton et al. [6] is 0.675. For the 28-day-old specimens of Alexander and Magee [25], the experimental results are plotted on both figures as the degree of hydration should be somewhere between the values of 0.6 and 0.675. The experimental results were then plotted along with the simulation data in Figs. 5 and 6. The agreement between experimental data and simulation results is quite reasonable for these two limited sets of data. For the experimental systems of Alexander and Magee [25], it would

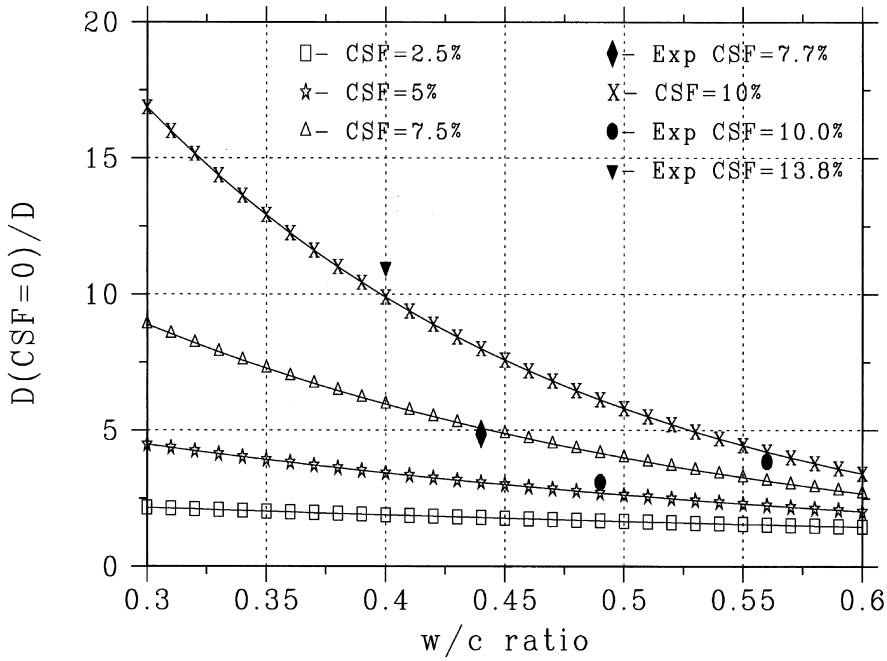

Fig. 6. Computed multiplicative increase in diffusion resistance due to silica fume addition vs. w/c ratio for an assumed degree of hydration of 0.675. Filled data points indicate the experimental data of Hooton et al. [6] (7.7% and 13.8%) and of Alexander and Magee [25] (10%).

be expected that the w/c = 0.49 specimens would have hydrated to a slightly lesser degree than the w/c = 0.56 specimens, hence, the observed agreement between the w/c = 0.49, α = 0.6 results and also between the w/c = 0.56, α = 0.675 results.

Several limitations must be kept in mind when considering the developed equation for predicting diffusivity. First, it assumes that the concrete is saturated and free from defects (such as cracking or other local inhomogeneities). Second, it also assumes that chloride ion transport is the only phenomenon occurring within the microstructure. The experimental results of Jensen [17] have indicated that when leaching (of calcium hydroxide and other components from the cement paste) and diffusion of chloride ions occur simultaneously, the measured diffusion coefficients are approximately a factor of 2.5 greater than those obtained under non-leaching conditions. Thus, the exact experimental conditions used for evaluating a concrete diffusivity have a major influence on the measured coefficients. If leaching conditions will be present in the actual concrete exposure, the coefficients predicted by Eq. (5) may need to be increased by up to a factor of 2.5, to provide a conservative estimate of field performance. Given the highly variable field exposure conditions, etc., it may be better to use the developed equation in a relative sense to predict the expected relative improvement in performance (service life) by the addition of silica fume to a base concrete mixture. Of course, Eq. (5) has been developed for w/c ratios between 0.3 and 0.5, silica fume additions between 0% and 10%, aggregate volume fractions between 0.62 and 0.70, and degrees of hydration between about 0.6 and 0.9. Extrapolation beyond this range of parameters using the developed equation may yield predictions of limited validity and should be performed only with extreme caution.

4. Conclusions

An equation has been developed for predicting the chloride ion diffusivity of high performance concretes containing silica fume as a function of mixture proportions and expected degree of hydration. The equation can be used in an absolute sense to predict the diffusivity of a specific concrete, or in a relative sense to estimate the improvement in diffusivity that can be achieved by the addition of silica fume to a concrete of known diffusivity. The model-predicted relative improvements appear to be in good agreement with the experimental data generated in two recent studies. Silica fume is observed to be particularly efficient in lower w/c ratio systems; for w/c = 0.3, a 10% silica fume addition may reduce diffusivity by a factor of 15 or more. Thus, *properly designed*, *placed*, and *cured* silica fume concretes should provide a substantial increase in the service life of steel-reinforced concretes in severe corrosion environments.

Acknowledgments

The author would like to thank the Partnership for High Performance Concrete Technology (PHPCT) program at NIST for funding this research.

References

[1] J.R. Clifton, L.I. Knab, Service life of concrete, NISTIR, 89-4086, US Department of Commerce, 1989.
[2] O.E. Gjorv, K.E. Loland, Condensed Silica Fume in Concrete, BML Report 82.610, The Norwegian Institute of Technology, 1982.
[3] O.M. Jensen, P.F. Hansen, Autogenous deformation and change of the relative humidity in silica fume modified cement paste, ACI Mater J 93 (6) (1996) 539–543.
[4] D.P. Bentz, V. Waller, F. deLarrard, Prediction of adiabatic temperature rise in conventional and high-performance concretes using a 3-D microstructural model, Cem Concr Res 28 (2) (1998) 285–297.
[5] N.S. Berke, L.R. Roberts, Use of Concrete Admixtures to Provide Long-Term Durability from Steel Corrosion vol. 119-20, ACI SP, Farmington Hills, MI, 1989, pp. 383–403.
[6] R.D. Hooton, P. Pun, T. Kojundic, P. Fidjestol, Influence of silica fume on chloride resistance of concrete, Proc. of the PCI/FHWA International Symposium on High Performance Concrete, 1997, pp. 245–256.
[7] V. Baroghel-Bouny, P. Rougeau, T. Chaussadent, G. Croquette, Etude Experimentale de la Penetration des Ions Chlorures dans Deux Betons B30 et B80 Durabilite des Betons LMDC, Toulouse, France, 1998, pp. 243–261.
[8] AASHTO T 277-83, Standard method of test for rapid determination of the chloride permeability of concrete, American Association of State Highway and Transportation Officials, Washington, DC, 1983.
[9] D.P. Bentz, E.J. Garboczi, E.S. Lagergren, Multi-scale microstructural modeling of concrete diffusivity: Identification of significant variables, Cem Concr Aggregates 20 (1) (1998) 129–139.
[10] D.P. Bentz, R.J. Detwiler, E.J. Garboczi, P. Halamickova, L.M. Schwartz, Multi-scale modelling of the diffusivity of mortar and concrete in: L.O. Nilsson, J.P. Ollivier (Eds.), Chloride Penetration into Concrete RILEM, Paris, France, 1997, pp. 85–94.
[11] D.P. Bentz, O.M. Jensen, A.M. Coats, F.P. Glasser, Influence of silica fume on diffusivity in cement-based materials: I. Experimental and computer modelling studies on cement pastes, Cem Concr Res 30 (2000).
[12] D.P. Bentz, Three-dimensional computer simulation of cement hydration and microstructure development, J Am Ceram Soc 80 (1) (1997) 3–21.
[13] D.P. Bentz, E.J. Garboczi, K.A. Snyder, A hard core/soft shell microstructural model for studying percolation and transport in three-dimensional composite media, NISTIR 6265, US Department of Commerce, January, 1999.
[14] B. Lu, S. Torquato, Nearest-surface distribution functions for polydispersed particle system, Phys Rev A 45 (1992) 5530–5544.
[15] E.J. Garboczi, D.P. Bentz, Multi-scale analytical/numerical theory of the diffusivity of concrete, Adv Cem Based Mater 8 (1998) 77–88.
[16] E.J. Garboczi, L.M. Schwartz, D.P. Bentz, Modelling the influence of the interfacial transition zone on the D.C. electrical conductivity of mortar, Adv Cem Based Mater 2 (1995) 169–181.
[17] O.M. Jensen, Chloride ingress in cement paste and mortar measured by electron probe micro analysis, Technical Report, Series R, No. 51, Technical University of Denmark, 1998.
[18] D.P. Bentz, C.J. Haecker, An argument for using coarse cements in high performance concrete, Cem Concr Res 29 (4) (1999) 615–618.
[19] D.P. Bentz, K.A. Snyder, P.E. Stutzman, Microstructural model-

ling of self-desiccation during hydration in: B. Persson, G. Fagerlund (Eds.), Self-Desiccation and Its Importance in Concrete Technology Lund Institute of Technology, Lund, Sweden, 1997, pp. 132–140.
[20] ASTM C-33, Standard specification for concrete aggregates Annual Book of ASTM Standards vol. 04.02, American Society for Testing and Materials, West Conshohocken, PA, 1997.
[21] J. Neter, W. Wasserman, M.H. Kutner, Applied Linear Statistical Models, Irwin, Boston, 1990.
[22] D.P. Bentz, E.J. Garboczi, Simulation studies of the effects of mineral admixtures on the cement paste–aggregate interfacial zone, ACI Mater J 88 (5) (1991) 518–529.
[23] N.R. Buenfeld, E. Okundi, Effect of cement content on transport in concrete, Mag Concr Res 50 (4) (1998) 339–351.
[24] J.D. Shane, T.O. Mason, H.M. Jennings, E.J. Garboczi, D.P. Bentz, Effect of the interfacial transition zone on the conductivity of portland cement mortars, J Am Ceram Soc (in press).
[25] M.G. Alexander, B.J. Magee, Durability performance of concrete containing condensed silica fume, Cem Concr Res 29 (6) (1999) 917–922.